Improving the fretting and corrosion fatigue performance of 300M ultra-high strength steel using the ultrasonic surface rolling process

Weidong Zhao, Daoxin Liu, Xiaohua Zhang, Ying Zhou, Ruixia Zhang, Hao Zhang, Chang Yé

Improving the fretting and corrosion fatigue performance of 300M ultra-high strength steel using the ultrasonic surface rolling process

Weidong Zhao[a,b], Daoxin Liu [a]*, Xiaohua Zhang[a], Ying Zhou[c], Ruixia Zhang[b], Hao Zhang[b], Chang Ye[b*]

[a] Corrosion and Protection Research Laboratory, Northwestern Polytechnical University, 127 You Yi Xi Road, Xi'an 710072, China;

[b] Department of Mechanical Engineering, The University of Akron, Akron, OH 44325, USA

[c] UMR CNRS 6226 Institut des Sciences Chimiques de Rennes, INSA Rennes, 20 Avenue des Buttes de Coësmes, 35708 Rennes Cedex 7, France

* Corresponding author e-mail addresses:

D.X. Liu: liudaox@nwpu.edu.cn; C. Ye: cye@uakron.edu

Abstract:

300M ultra-high strength steels (300M steels) are frequently used in the manufacture of aircraft landing gear due to their high strength and ductility. However, their high sensitivity to surface defects accelerates fatigue failure and hinders their wider application. In this work, ultrasonic surface rolling processing (USRP) was used to process 300M steel. The surface roughness, hardness, microstructure, and residual stresses before and after USRP treatment were compared, and the surface roughness for USRP-treated samples (0.062 μm) was found to be lower than that for untreated samples (0.32 μm). In addition, a plastically deformed layer was generated on the surface of USRP-treated samples that resulted in higher hardness. Beneficial compressive residual stresses were introduced as a result of USRP treatment. The better surface finish, higher surface hardness and compressive residual stresses lead to significant improvement in the resistance of the 300M steels to fretting fatigue and corrosion fatigue. The fretting fatigue life increased from 11.9K cycles to 56.3K cycles, while the corrosion fatigue life increased from 29.9K cycles to 702.1K cycles.

Keywords: 300M ultra-high strength steels; Ultrasonic surface rolling process (USRP); Compressive residual stress; Corrosion Fatigue; Fretting fatigue

1. Introduction

Compared with common steels, 300M ultra-high-strength steels have extremely high tensile strength (~1900 MPa) and yield strength (~1600 MPa) and thus are commonly used in the manufacture of aircraft landing gear. Landing gear requires high fretting fatigue strength to

withstand a high number of takeoffs and landings. In coastal areas, fatigue damage to the landing gear is exacerbated by corrosion damage induced by ocean air and seawater. Thus, damage due to fretting fatigue (FF) [1] and corrosion fatigue (CF) [2] can reduce the service life of the landing gear. Fatigue crack nucleation and the growth of defects, which frequently occur at the material surface, can be increased by fretting wear and corrosion damage. However, Sih and Macdonald [3] indicated that 300M steel is very sensitive to surface defects. If the surface of landing gear made from 300M steel is damaged, the fatigue crack nucleation rates will be further increased. Therefore, an effective surface modification technique for decreasing surface defects and improving the fatigue life of 300M steel is desperately needed.

Surface mechanical strengthening methods are frequently used to increase fatigue resistance of metallic materials by changing the surface microstructure and the distribution of residual stresses [4–8]. For example, Prevéy et al. [9] reported that low plasticity burnishing technology can effectively improve the high cycle CF strength of 300M steel by generating high surface compressive residual stress. Bertini and Santus [10] used deep rolling (DR) technology to generate a smooth surface and residual stresses that significantly increased the FF properties of 7075 aluminum alloy. In the fields of aviation and machining, shot peening (SP) is widely used because it can effectively increase fatigue resistance and is easy to implement [11–13]. Namjoshi et al. [14] illustrated that SP effectively impeded the FF micro crack nucleation from the surface of Ti6Al4V by transforming tensile residual stress to compressive residual stress. Majzoobi and Abbasi [15] also observed that SP could remarkably increase the FF resistance of an aluminum alloy. However, Tekeli [16] found that SP could damage the surface of steel by subjecting it to impacts from non-uniform shot blasting. Zhang and Liu [17] also observed that SP increased surface roughness and generated some micro-cracks in the surface of Ti811. This shortcoming of SP limits its use in treating 300M steel. Traditional SP by itself cannot meet the requirements for fewer surface defects and a deeper strengthening of the surface layer in 300M steel.

Ultrasonic surface rolling processing (USRP) is a recently developed technology that combines the advantages of traditional rolling technology with ultrasound technology [18–20]. Compared with a traditional rolling technique, USRP relies mainly on ultrasonic energy instead of using force to treat the surface of a sample, forming a deeper plastic deformation layer at the sample surface by using a lower load. For instance, Liu et al. [21] noted that the surface grains of 40Cr steel were severely refined after USRP treatment. Li et al. [22] also reported that USRP is able to induce plastic deformation and compressive residual stresses in the surface of Ti6Al4V that can significantly improve the fretting friction and wear resistance. In addition, because the loading in USRP is much lower than that used in traditional rolling technology, no changes in the overall size and shape of a sample will occur. Wang et al. [23] also reported that USRP decreased the surface roughness of X80 steel from 1.3 μm to 0.2 μm. The reason is that during USRP treatment, the sample surface is struck by a freely rotating ball in a liquid lubricant, which can reduce surface defects and achieve a much smoother surface. Compared with SP—which is conducted using an automated shot peening machine and may not strike recessed areas on the surface or other areas that are difficult to reach—USRP equipment can be installed on a computer numerical control (CNC) lathe, allowing the surface of the sample to be treated homogeneously by accurately controlling the strike intensity and density. At present, many

studies try to use USRP to change the surface state and mechanical properties of metal materials. Lu et al. [24] reported that USRP significantly increased the surface finish and compressive residual stress and hardness of aluminum. Wang et al. [25] used USRP technology to treat Ti6Al4V, which significantly enhanced the surface hardness and wear resistance. In summary, USRP technology has obvious advantages in improving surface finish and mechanical properties of some metallic materials.

USRP technology has been widely used in materials that are soft to moderately hard, such as titanium alloy and aluminum alloy, to improve the mechanical properties. However, no studies have used USRP treatment to decrease surface defects on 300M steel, a material that is typically difficult to deform. Specifically, the relationship between surface integrity (surface finish, microstructure, residual stress, etc.) and mechanical behaviors (FF and CF) of 300M ultra-high-strength steel after USRP treatment has not been investigated in any studies published in the literature to date. In this study, we report the impact of USRP on surface defects and the mechanical performance (in terms of FF and CF) of 300M steel. The surface microstructure and distribution of surface hardness and residual stress of 300M steel were also characterized.

2. Experimental Materials and Methods

2.1. Ultrasonic Surface Rolling Process treatment

By combining ultrasonic striking and static load, as shown in Fig. 1, USRP treatment can produce a plastic deformation layer in the surface of a target sample by using a tungsten carbide cobalt (WC/Co) ball (with a diameter of 14 mm) that freely rotates at high speed to strike and roll the surface. In this study, an ultrasonic frequency of 28 kHz, a vibration amplitude of 12 μm and a static load of 900 N were used. To process the surface of a rod-shaped sample, the USRP equipment was mounted on a CNC lathe. A rotation speed of 45 r/min and a feed rate of 0.08 mm/min were used in this study.

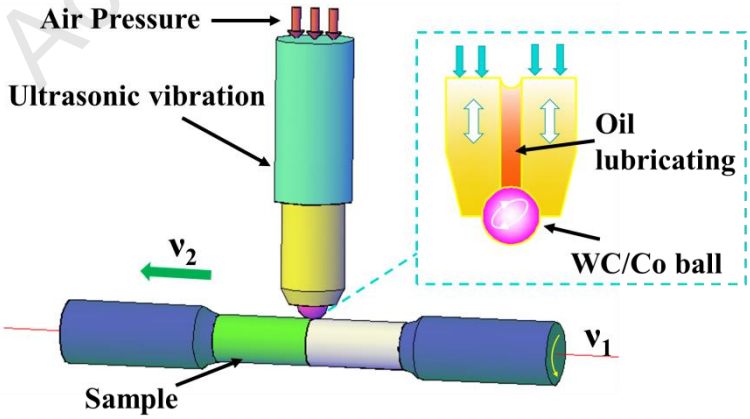

Fig. 1. Schematics of the USRP test setup (inset adopted from Liu et al. [26]).

2.2. Materials

Table 1 exhibits the chemical composition of the 300M steel. After double annealing (at 870°C for 30 min, followed by cooling in oil at 300°C for 2 h, followed by air cooling), the main microstructure of 300M steel was found to be tempered martensite; very few bainites and residual austenites were observed in the microstructure. As shown in Table 2, the 300M steel showed great strength and ductility.

Rod-shaped samples were prepared for tests to determine FF and CF (Fig. 2). To ensure a certain contact strength between the fatigue sample and the fretting pads, the fretting pads were also made of 300M steel. The surface roughness for all samples was 0.32 μm as produced by sequential mechanical polishing using different grades of silicon carbide sandpaper (#320, #400, #600, #800, #1000 and #1200).

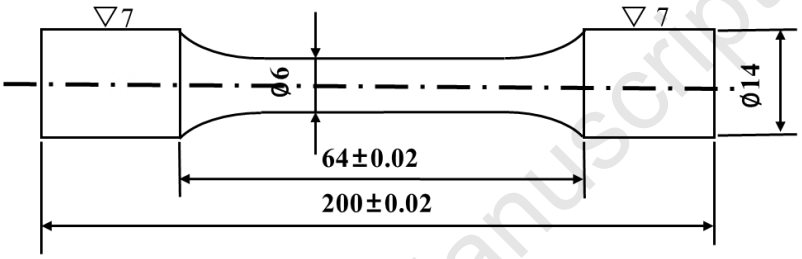

Fig. 2. Dimensions of samples for fretting fatigue and corrosion fatigue (in mm).

Table 1. Chemical composition of 300M steel (wt.%)

Carbon (C)	Chromium (Cr)	Vanadium (V)	Manganese (Mn)	Silicon (Si)	Nikel (Ni)	Molybdenum (Mo)	Copper (Cu)	Iron (Fe)
0.42	0.84	0.09	0.82	1.57	1.94	0.38	0.84	Bal.

Table 2. Mechanical properties of 300M steel after double annealing

Yield strength (MPa)	Tensile strength (MPa)	Elongation (%)	Section shrinkage (%)
1631	2015	12.3	52.8

2.3. Testing and characterization methods

The following tests were conducted to determine the surface integrity and mechanical properties of the USRP-treated 300M samples:

- Microstructure characteristics: Microstructure characteristics of USRP-treated samples were determined by using a JEOL JSM-6390 scanning electron microscope (SEM) at 20 kV. The cross sections of the samples were mechanically polished using silicon carbide sandpaper (#300, #400, #600, #800 and #1200) and diamond suspensions (3 μm and 1 μm). After polishing, each sample was etched using a 4% nital solution.

- Identification of phase composition: A Rigaku D/Max 2200 PC X-ray diffraction (XRD) unit was used to identify surface phase changes in untreated and UNSM-treated samples at 40 kV and 40 mA. The test conditions were as follows: copper was used as the radiation source, and the XRD scanning was conducted at a 2θ angle ranging from 30° to 85° at a rate of 1 degree/minute.
- Surface morphology and roughness: The surface fluctuation and unevenness of 300M steel before and after USRP treatment were investigated by using SEM (JEOL JSM-6390 microscope). A TR-300 surface roughness tester from Time Instrument Indonesia was also applied to further study the surface state changes.
- Residual stress: A Proto LXRD-MG2000 residual stress tester was utilized to analyze the residual stress of 300M steel before and after USRP treatment by the classical $\sin^2\Psi$ method. The test conditions were as follows: the target radiation was Cr (30 kV, 8 mA) and the diffraction crystal surface was (211). To measure the in-depth residual stresses, all samples were electrochemically polished using a solution of 25% H_2SO_4+65% H_3PO_4 +10% H_2O at a temperature of 60°C and a rate of 5 μm/min). The X-ray beam size was Φ 3 mm and the area of area of electro-polishing was 94.2 mm^2.
- Hardness: The micro-hardness in the cross section of untreated and USRP-treated samples was measured using a Knoop HV-1000 micro-hardness tester. All samples were tested under a load of 25 g at a dwell time of 20 s. Each measurement was repeated at least five times.
- Fretting fatigue: A self-designed experimental apparatus was used to carry out FF testing in an SDS100 electro-hydraulic servo fatigue tester. The loading method was set as pull-pull. As shown in Fig. 3, the form of contact between the sample and fretting pad was cylinder to camber. The fatigue cyclic loading waveform was a sine wave of 10 Hz. The contact force between the sample and the fretting pad was imposed by a bolt and was controlled at 200 MPa. The contact pad, which is also made from 300M steel, was polished using carbide sandpapers (from 300# to 1200#). The contact pad had a surface roughness *Ra* of 0.118 μm and a surface hardness of 647 HK. The constant stress ratio *R* was 0.1, and the maximum axial cycle stress σ_{Max} was 1100 MPa. The number of cycles before the sample fracture was used to evaluate the FF resistance of the 300M steel samples. Each measurement was repeated three times. To investigate the mechanism of FF fracture, the fatigue fracture surface features were studied using SEM.

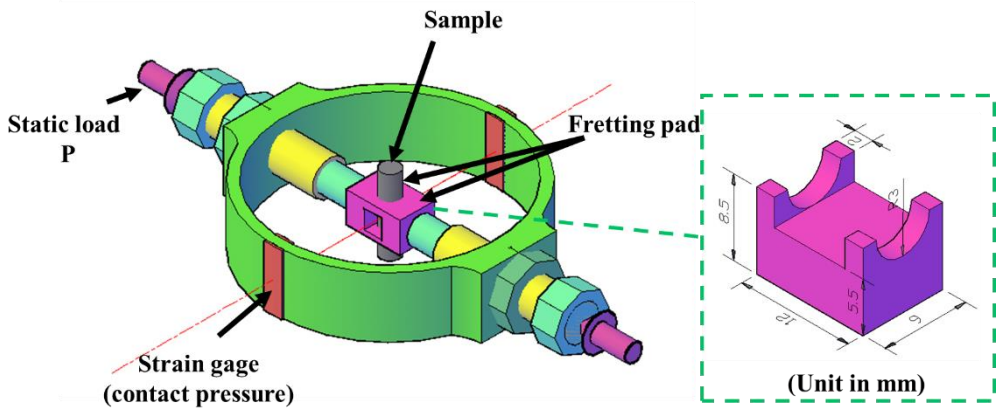

Fig. 3. Schematic diagram of the fatigue fracture testing system (inset adopted from Liu et al. [26]).

- Corrosion fatigue: To determine corrosion fatigue performance, each 300M sample was fixed on the self-designed CF testing system, which consisted of a SDS100 electro-hydraulic servo fatigue tester and a glass container that was used to hold an aqueous solution of 3.5% NaCl. Fig. 4 presents a schematic diagram of the CF test setup. The gauge section of the sample was completely submerged in the solution, and the ratio of the volume of the corrosion solution to the surface area of the gauge section was not less than 20 mL/cm^2. The CF test was carried out at 24 ± 3°C using a pull-pull axial loading mode. The fatigue cyclic loading waveform was a sine wave, and the axial loading force was 1100 MPa. The uniform frequency was 10 Hz, and the stress ratio *R* was 0.1. Each measurement was repeated three times. After CF testing, selected fracture surfaces were analyzed using SEM.

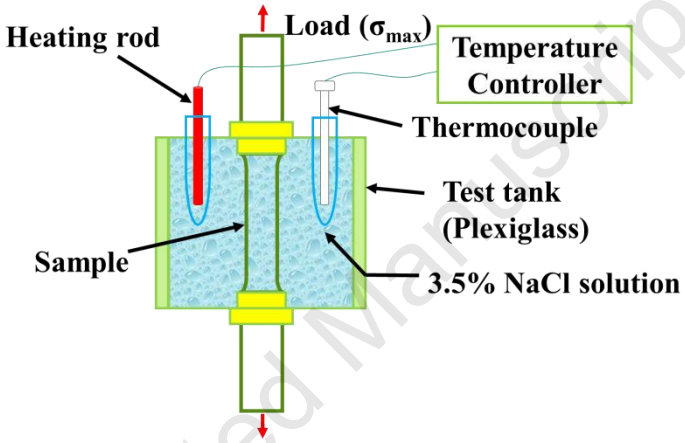

Fig. 4. A schematic diagram of the CF testing system.

3. Results and discussion

3.1 Surface morphology and roughness

The surface state of untreated and USRP-treated 300M steel samples are presented in Fig. 5. The untreated samples were mechanical polished using a grinder to obtain low surface roughness (~ 0.3 μm). Obvious grooves can be noticed in the surface of the untreated sample, and these grooves contribute to the initiation of fatigue cracking. After USRP treatment, most mechanical scratches on the surface of the samples were noted to have healed, and the number of surface defects were dramatically reduced. The surface roughness *Ra* of untreated samples is 0.32 μm (as shown in Fig. 5c). Following USRP treatment, the sample surface has become much smoother, and the surface roughness is decreased to 0.062 μm. Because the loading in USRP is much lower than that used in traditional rolling and the ball in USRP is able to freely rotate over the surface of sample, any micro-pits and mechanical furrows in the surface can be flattened.

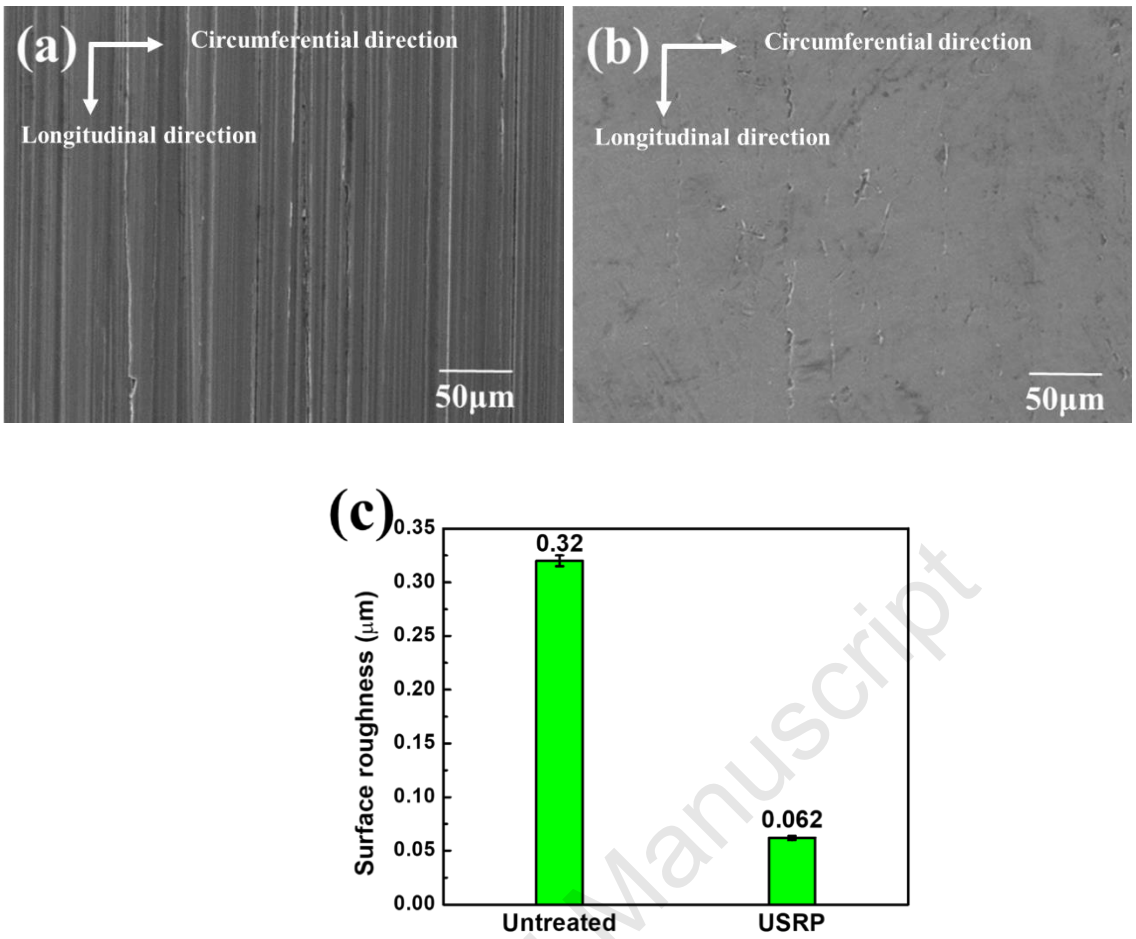

Fig. 5. The surface morphology of 300M steel (a) before and (b) after USRP treatment. (c) Surface roughness of 300M steel before and after USRP treatment.

3.2 Microstructure

SEM micrographs of the cross sections of 300M steel samples before and after USRP treatment are shown in Fig. 6. Before USRP treatment, a martensitic structure with different orientations can be observed. After USRP treatment, a plastic deformation layer can be observed with the martensite laths aligned in the scanning direction. The thickness of the severe plastic deformed layer is about 6 μm (Fig. 6b). Wang et al. [27] observed similar surface microstructure in USRP-treated 40Cr steel. However, due to the severe surface deformation, it was difficult to determine the grain size.

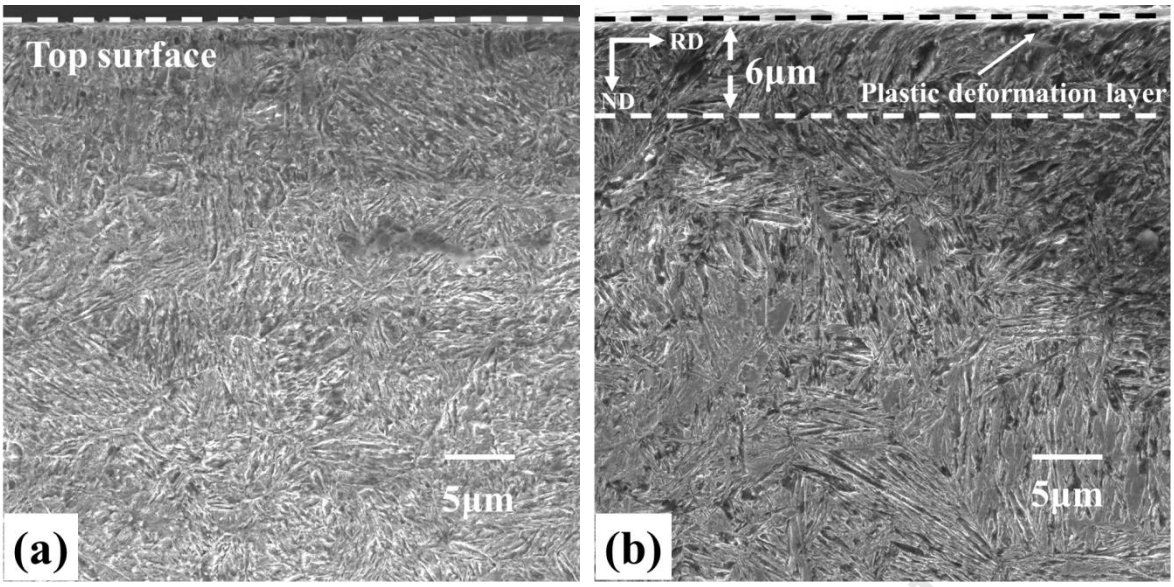

Fig. 6. The cross-sectional microstructure of 300M steel (a) before and (b) after USRP treatment (where RD is the rolling direction and ND is the normal direction).

3.3 XRD

Figure 7 shows the change in the XRD patterns of 300M steel samples before and after USRP treatment. After USRP treatment, the three main peaks at (100), (200) and (211) become much lower and wider, and the relative intensities of the three peaks are also decreased. At the same time, USRP is able to refine the microstructure and induce surface compressive residual stress on the samples by striking the sample surface at high frequency; as a result, the (100), (200) and (211) peaks are shifted to the right following USRP. To facilitate a further comparison of the XRD images obtained before and after USRP treatment, the full width at half maximum (FWHM) values were determined (Table 3). From Table 3, it can be noticed that the FWHM values of the three XRD peaks were slightly increased after USRP treatment, indicating a reduction in the surface grain size and an increase in the surface dislocation density following USRP.

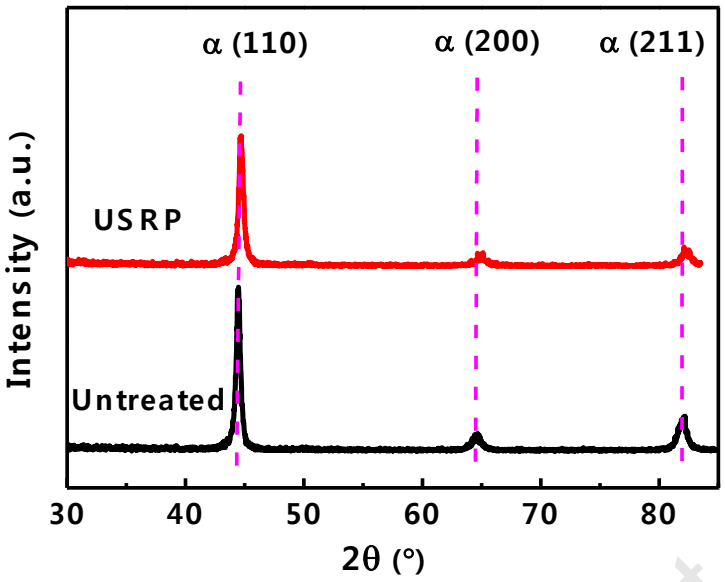

Fig. 7. XRD patterns of 300M steel before (untreated) and after USRP treatment.

Table 3. FWHM values of the main peaks identified from XRD patterns of 300M steel

Crystal plane	Untreated	USRP
(110)	0.433	0.443
(200)	0.531	0.547
(211)	0.629	0.635

3.4 Hardness

Figure 8 compares the hardness of the 300M steel samples before and after USRP treatment. The mean hardness at the top surface of the untreated samples is 644 HK, while that for samples after USRP treatment is 876 HK, corresponding to a 36% increase. At the same time, in the direction along the cross section, the hardness of the USRP-treated samples gradually decreases. The work-hardening and grain refinement induced by the plastic strain results in an improvement in hardness. Due to the gradient nature of the plastic strain induced by USRP, the plastic strain in the top surface is also the highest and decreases gradually with depth; thus, the hardness in the top surface is the highest and decreases gradually with depth. In addition, Carlsson and Larsson [28] reported that residual stress also affects the surface hardness. USRP can induce high-magnitude compressive residual stress in the top layer; this also contributes to the increase in hardness. It should be noted that the hardened layer is around 140 μm, while the obvious plastic deformation layer is only 6 μm (Fig. 6). The actual work-hardened layer can be much deeper than the depths that can be observed using SEM. Similar hardening behavior has been observed when using USRP or other mechanical surface strengthening methods for treating other metals [24,29–32].

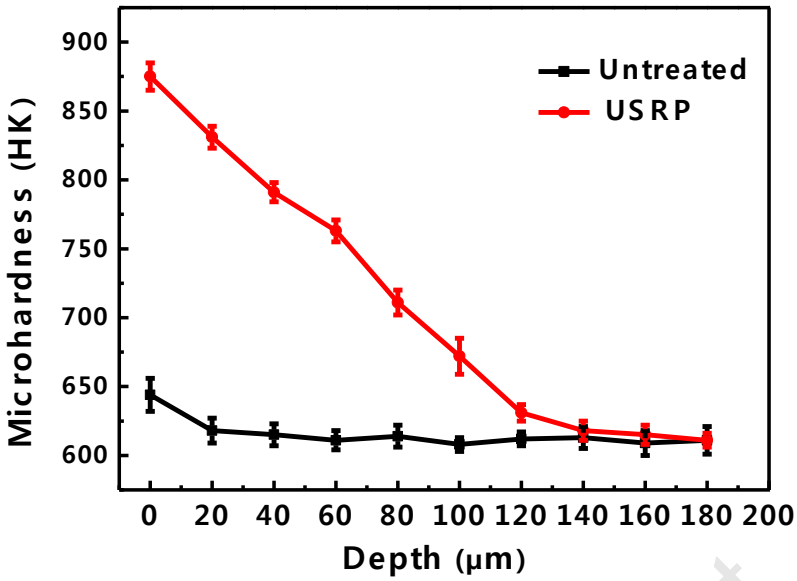

Fig. 8. In-depth hardness of 300M steel before and after USRP treatment.

3.5 Residual stress

Figure 9 presents the change of in-depth compressive residual stresses in 300M steel before and after USRP treatment. It can be observed that the un-treated specimen is almost stress-free while a deep layer of compressive residual stresses was introduced in the USRP-treated specimen. The mean compressive residual stress on the top surface increases to 1285 MPa, and the depth of surface compressive residual stress layer is 520 μm. Similar to the results of other studies [20,33,34], USRP was found to produce a large and deep layer of compressive residual stress. Even though the residual stress introduced has some effect on the hardness [28], the effect if not that significant compared with that by grain refinement and work-hardening. The increased hardness is mainly attributed to microstructure refinement and work hardening. Because of the low microstructure refinement and work hardening at locations farther below the top surface, the hardened layer is not as deep as the layer with compressive residual stress. In addition, based on the Hertz contact model, the area of maximum shear stress is located in the subsurface, and the maximum compressive residual stress of the USRP-treated specimen is found at a depth of 20 μm below the top surface.

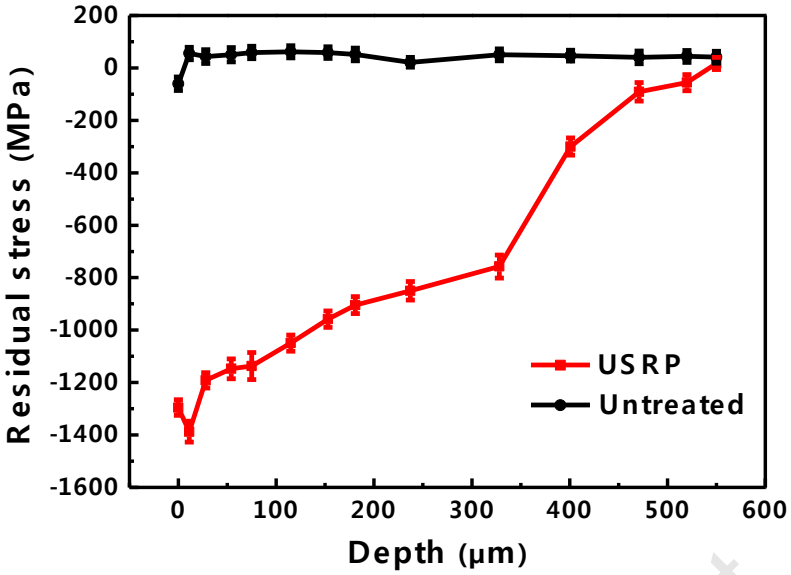

Fig. 9. Compressive residual stress of 300M steel before and after USRP treatment.

3.6 Fretting fatigue test

FF testing was carried out to evaluate the FF resistance of 300M steel before and after USRP treatment. Fig. 10 shows the average FF life of 300M steel before and after USRP treatment (σ_{max}= 1100 MPa). The mean number of FF cycles before failure for the three untreated samples is 11.9×10^3. For USRP-treated samples, the mean number of FF cycles is 56.3×10^3, corresponding to a 4.7-fold increase. These results demonstrate that the FF resistance of 300M steel was significantly enhanced by USRP treatment.

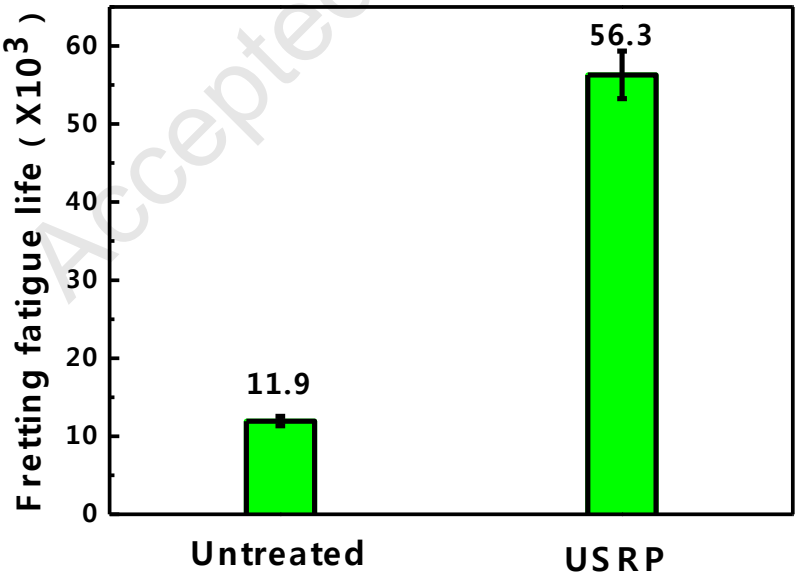

Fig. 10. The number of cycles until FF failure (σ_{max}= 1100 MPa) of 300M steel before (untreated)
and after USRP treatment.

The improvement in the FF properties of 300M steels following USRP treatment is attributed to three main causes. First, the enhancement of surface hardness after USRP treatment is an

important reason for the improvement of the FF properties of 300M steel by hindering FF crack nucleation. Generally, FF crack nucleation is caused not only by the fretting wear damage but also by the high concentration of stress near the contact edge [35,36]. It is important to note that the enhanced hardness can simultaneously improve the resistance of fretting wear damage and the concentration of stress. On one hand, the improvement of surface hardness can significantly reduce the fretting wear damage. Because the fretting pads are also made from 300M steel, the surface hardness of USRP-treated samples is higher than that of fretting pads. Hence, the fretting wear damage of the USRP-treated samples against the fretting pad is much less than that of untreated samples against the fretting pad. On the other hand, the stress concentration at the contact edge is also decreased by improved hardness. In general, hardness is proportional to the yield strength of metallic materials [37]. Due to the formation of a hardening layer on the surface of USRP-treated samples, the surface local yield strength is also improved. Enhanced surface yield strength can improve the stress concentration resistance of metallic materials [38]. Therefore, the surface of a USRP-treated sample has a lower stress concentration at the contact edge than that of the untreated sample. In summary, the higher hardness of the USRP-treated sample is able to slow FF crack initiation from the fretting wear and stress concentration zone.

Second, the introduction of compressive residual stress after USRP treatment can hinder FF crack nucleation and early crack propagation, which is another important reason for the improved FF properties of 300M steel. First, the compressive residual stress reduces the FF crack nucleation rate for the following two reasons: 1) It was reported that the surface residual compressive stress not only weakens the effective fretting fatigue that drives stress and stress concentration [39,40], but it also slows fretting wear [41,42]. Reduced stress concentration and fretting wear damage is conducive to the inhibition of FF crack nucleation, and 2) According to prior studies [15,43], induced compressive residual stresses can enhance the tangential force threshold level. When the tangential force is below a certain threshold level, there will be no FF crack nucleation at the trailing edge of contact. Due to the formation of a larger and deeper layer of compressive residual stress at the surface, the USRP-treated samples require a larger tangential force to promote FF crack nucleation. Hence, the induced compressive residual stress after USRP treatment contributes to the slowing of the FF crack nucleation. In addition, it has been reported that the major contribution of compressive residual stress is to prevent early FF crack propagation [15,44]. In the early FF crack propagation stage, compressive residual stress can significantly decrease tensile stress at the crack tip [44]. Similar to clamping stress, compressive residual stress can also close up FF cracks in the early stages of FF crack propagation [45]. Therefore, the early FF crack propagation rate is significantly reduced by the induction of large compressive residual stress in the near-surface region after USRP treatment [46–49]. In summary, the compressive residual stress introduced by USRP treatment can improve the FF resistance of 300M steel.

Finally, many studies have reported that the surface roughness has a more complex influence on the FF properties of materials [17,44,50]. To study the influence of surface roughness on FF, surface roughness in the fretting wear zone of all samples was also measured after FF testing. The surface roughness (*Ra*) of both untreated and USRP-treated samples after FF

testing is enhanced (0.44 μm and 0.188 μm, respectively). However, the surface roughness of untreated samples is always larger than that of USRP-treated samples before and after FF testing. This proves that reduced surface roughness also has a positive influence on the improvement of FF properties, since fretting fatigue cracking has been reported to be easily initiated at the location of maximum stress–strain (a location near the contact edge), which mainly depends on the tangential stress induced by fretting action on the contact interface of the contact pad and the sample [35]. In the actual fretting action process, the fretting pad and sample only have some points of contact rather than complete contact. When the surface roughness of a sample decreases, there will be a larger number of real contact points between the fretting pad and sample, which can reduce the real contact pressure [34]. As a result, adhesion damage will be inhibited, and the tangential stress of USRP-treated samples induced by fretting action will also be decreased. Therefore, the enhanced surface roughness in the USRP-treated sample is also attributed to the increase in FF resistance.

The morphologies of the FF fracture and fretting wear zone of untreated and USRP-treated 300M steel (σ_{max}= 1100 MPa) can be observed in the SEM images presented in Fig. 11. The main FF cracks on all samples are detected at the fretting contact edge, where the maximum value of tangential stress and severe fretting wear is found [35,51]. Many obvious grooves, adhesions and fatigue cracks can be observed in the fretting wear zone of the untreated samples (Fig. 11a). The fretting damage mechanisms in the untreated 300M steel samples are adhesive wear, abrasive wear and fatigue wear. Following USRP treatment, the hardness of the USRP-treated samples is higher, so there are fewer grooves in the surface of the fretting wear zone (Fig. 11c). The surface damage mechanisms in the fretting wear zone of the USRP-treated samples are adhesive wear and fatigue wear only (with no abrasive wear). Severe wear damage occurred at the surface of untreated samples in the fretting wear zone, which provides numerous sites for fatigue crack nucleation. In Fig. 11b, many fatigue crack sources can be seen following FF fracture of untreated samples, which demonstrates that the life of FF is significantly controlled by the FF crack nucleation stage. Once these cracks generate from the surface, they expand rapidly and cause fatigue fracture. Compared with untreated samples, USRP-treated samples have fewer surface defects and larger compressive residual stresses that decrease the fatigue crack nucleation rate, such that only one fatigue crack was found in the USRP-treated sample (Fig. 11d). In other words, the fatigue life of 300M steel samples after USRP treatment is improved due to the decrease in surface defects and the induction of larger surface compressive residual stresses and higher surface hardness.

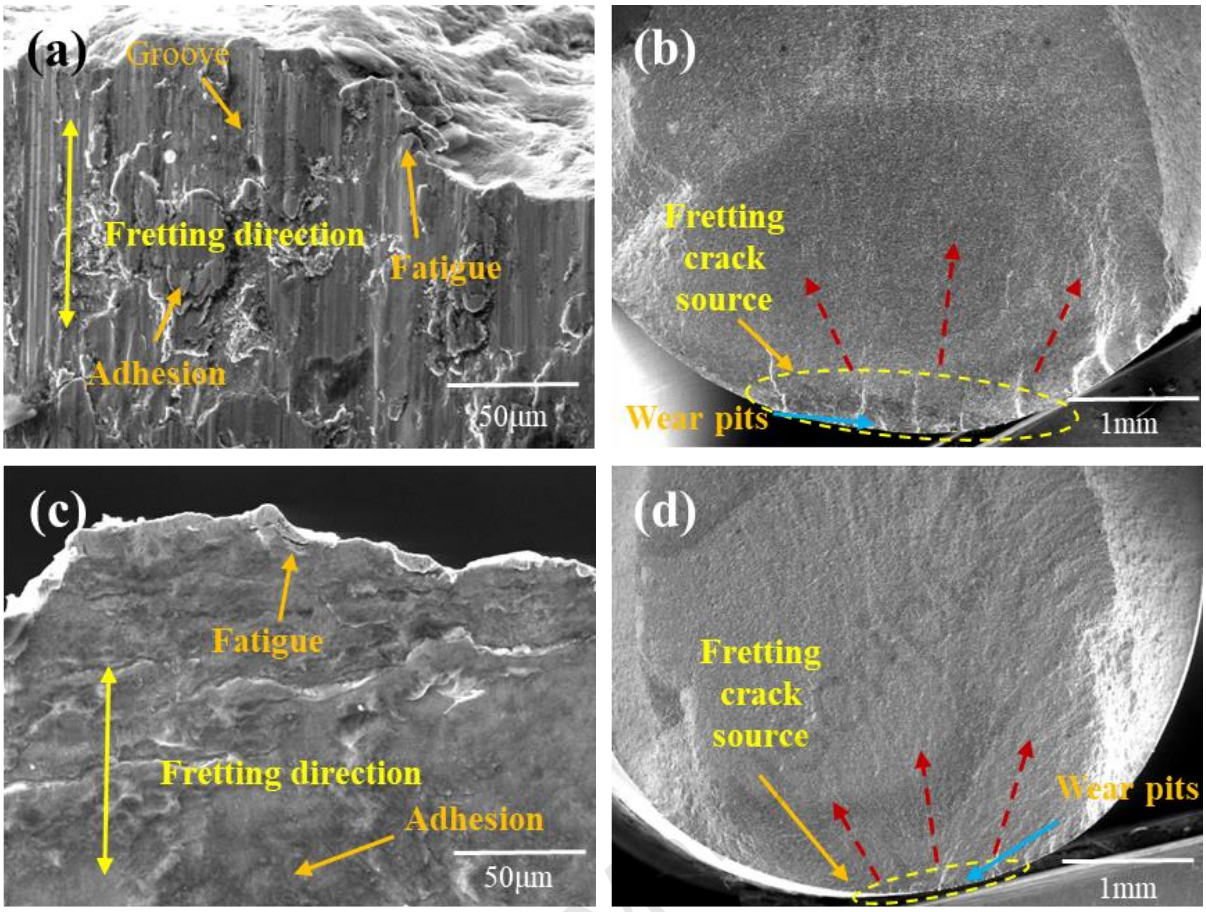

Fig. 11. Fatigue fracture SEM images of 300M steel before and after USRP treatment (maximum stress level σ_{max}=1100 MPa): The fretting wear zone of an untreated sample, (b) the FF fracture of an untreated sample, (c) the fretting wear zone of a USRP-treated sample, and (d) the FF fracture of USRP-treated sample.

3.7 Corrosion fatigue test

The CF test was performed in 3.5% sodium chloride solution to evaluate the CF properties of 300M steel before and after USRP. The average CF life of untreated and USRP-treated 300M steels (σ_{max}= 1100 MPa) is illustrated in Fig. 12. After repeating three parallel tests, the number of CF cycles (which represent the CF resistance) was recorded for untreated and USRP-treated samples. The mean number of CF cycles for untreated 300M steel samples is 29.9×10^3. For USRP-treated samples, the mean number of CF cycles, which is 702.1×10^3, represents a 23-fold increase over the number of cycles for untreated samples. This demonstrates that the tendency of USRP to decrease the surface corrosion activity by reducing surface defects is a major reason for the improvement in CF life in the USRP-treated samples.

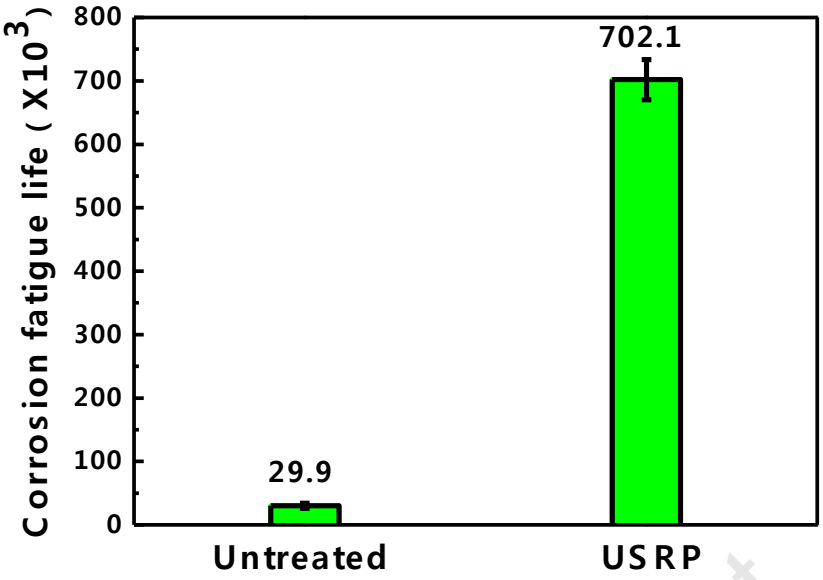

Fig. 12. The number of cycles before CF failure of 300M steel before (untreated) and after USRP treatment.

There are two main reasons for the increase in CF resistance of 300M steel in USRP-treated samples. On one hand, USRP can decrease surface defects by producing a sample surface with uniform electrochemical activation. Zuo et al. [52] have reported that the ratio *w*/*d* (where *w* and *d* indicate the mean width and mean depth of the grooves in the sample surface, respectively) can be used to evaluate the capability of corrosion pits to nucleate. With a decrease in roughness, the *w*/*d* ratio increases and corrosion pits in the sample surface become more difficult to nucleate. USRP can flatten the sample surface, which reduces the surface roughness. Compared with untreated samples, nucleation of corrosion pits on the surface of USRP-treated samples becomes more difficult, so the process of fatigue crack nucleation from corrosion pits is also restricted. On the other hand, if some fatigue micro-cracks are able to nucleate from the corrosion pits of USRP-treated 300M steel, the deeper and larger compressive residual stresses can heal the micro-cracks and hinder their further expansion. Thus, the CF resistance of 300M steels can be significantly enhanced by USRP. Due to the different failure mechanisms of FF and CF, FF will more easily damage the surface of USRP-treated samples and release the surface residual stresses than CF. Thus, compared with the FF life, the improvement in the CF life of USRP-treated sample is more obvious.

The morphologies of the CF fracture of 300M steel before and after USRP treatment (σ_{max}= 1100 MPa) are shown in Fig. 13. Numerous corrosion pits can be observed in the untreated samples (Fig. 13a). Because of the ubiquity of surface defects, the surface electrochemistry of the untreated samples is not uniform, and corrosion pits can easily nucleate from these defects. When the metal is subjected simultaneous alternating loading and corrosion attack, corrosion pits will lead to stress concentration, such that fatigue micro-cracks can be easily initiated from these areas. Thus, numerous fatigue cracks can be observed in the surface of the untreated samples (Fig. 13b). Compared with untreated samples, USRP-treated samples have only one fatigue crack source in the CF fracture (Fig. 13c, d). Moreover, the CF crack that initiated from the corrosion pits is delayed for a distance of ~120 μm. Because

electrochemical activation at the surface decreases after USRP treatment, the process of corrosion pit nucleation is prolonged. At the same time, the larger surface compressive residual stresses in the USRP-treated sample also hinder fatigue crack nucleation from corrosion pits and can delay the propagation of fatigue cracks into the interior of the sample. Therefore, after USRP treatment, it is obvious that the CF resistance of 300M steel can be enhanced by decreasing the surface roughness and increasing the surface compressive residual stresses.

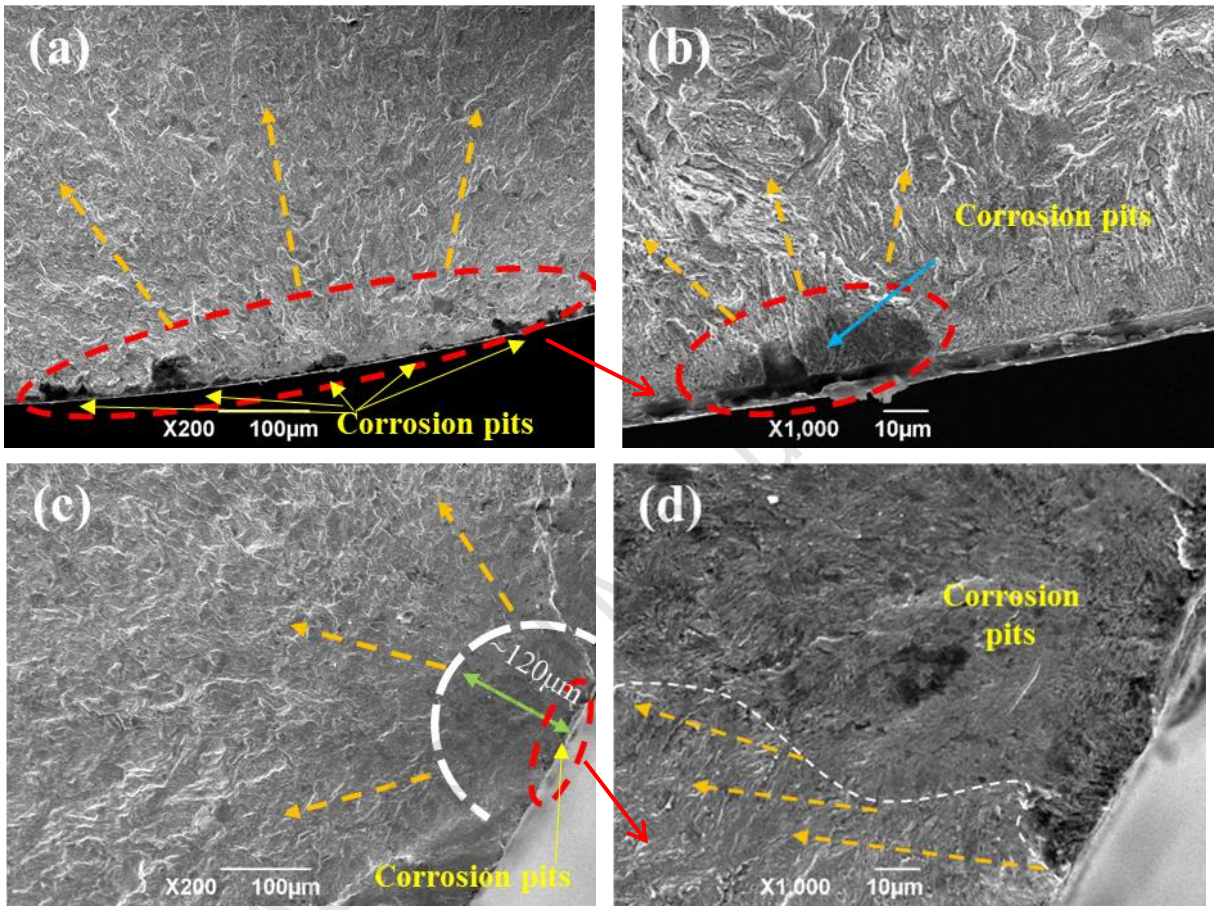

Fig. 13. Corrosion fracture SEM images of 300M steel before and after USRP treatment (maximum stress level σ_{max} = 1100 MPa): (a,b) The CF fracture of an untreated sample; (c,d) CF fracture of a USRP-treated sample.

4. Conclusion

In this study, USRP was used to decrease surface defects and improve the FF and CF resistance of 300M steel. The results demonstrate that USRP, by combining traditional rolling technology with ultrasound techniques, can significantly reduce surface defects in 300M steel and induce a surface strengthening layer, adjusting the distribution of residual stress and hardness. Following USRP treatment, the FF and CF properties of 300M steel are also improved, resulting from the reduction in surface defects and the increase in compressive residual stress and hardness. This research proves that USRP can potentially be used to treat 300M steel components for improved properties and performance in industrial applications.

Acknowledgments:

This work was supported by the National Natural Science Foundation of China (Award no. 51771155) and China Scholarship Council (CSC).

Reference

[1] Winkler J, Georgakis CT, Fischer G. Fretting fatigue behavior of high-strength steel monostrands under bending load. International Journal of Fatigue 2015;70:13–23. doi:10.1016/j.ijfatigue.2014.08.009.

[2] Pérez-Mora R, Palin-Luc T, Bathias C, Paris PC. Very high cycle fatigue of a high strength steel under sea water corrosion: A strong corrosion and mechanical damage coupling. International Journal of Fatigue 2015;74:156–65. doi:10.1016/j.ijfatigue.2015.01.004.

[3] Sih GC, Macdonald B. Fracture mechanics applied to engineering problems-strain energy density fracture criterion. Engineering Fracture Mechanics 1974;6:361–86. doi:10.1016/0013-7944(74)90033-2.

[4] Zhou J, Sun Z, Kanouté P, Retraint D. Effect of surface mechanical attrition treatment on low cycle fatigue properties of an austenitic stainless steel. International Journal of Fatigue 2017;103:309–17. doi:10.1016/j.ijfatigue.2017.06.011.

[5] Ganesh P, Sundar R, Kumar H, Kaul R, Ranganathan K, Hedaoo P, et al. Studies on fatigue life enhancement of pre-fatigued spring steel specimens using laser shock peening. Materials and Design 2014;54:734–41. doi:10.1016/j.matdes.2013.08.104.

[6] Kattoura M, Mannava SR, Qian D, Vasudevan VK. Effect of laser shock peening on residual stress, microstructure and fatigue behavior of ATI 718Plus alloy. International Journal of Fatigue 2017;102:121–34. doi:10.1016/j.ijfatigue.2017.04.016.

[7] Majzoobi GH, Azadikhah K, Nemati J. The effects of deep rolling and shot peening on fretting fatigue resistance of Aluminum-7075-T6. Materials Science and Engineering: A 2009;516:235–47. doi:10.1016/j.msea.2009.03.020.

[8] Ye C, Suslov S, Kim BJ, Stach EA, Cheng GJ. Fatigue performance improvement in AISI 4140 steel by dynamic strain aging and dynamic precipitation during warm laser shock peening. Acta Materialia 2011;59:1014–25. doi:10.1016/j.actamat.2010.10.032.

[9] Prevéy PS, Jayaraman N, Ontko N, Shepard M, Ware R, Coate J. Mitigation of Scc and Corrosion Fatigue Failures in 300M Landing Gear Steel Using Mechanical Suppression. Proceedings of the 6th Aircraft Corrosion Workshop 2004:1–12.

[10] Bertini L, Santus C. Fretting fatigue tests on shrink-fit specimens and investigations into the strength enhancement induced by deep rolling. International Journal of Fatigue 2015;81:179–90. doi:10.1016/j.ijfatigue.2015.08.007.

[11] Naidu NKR, Raman SGS. Effect of shot blasting on plain fatigue and fretting fatigue behaviour of Al-Mg-Si alloy AA6061. International Journal of Fatigue 2005;27:323–31. doi:10.1016/j.ijfatigue.2004.07.007.

[12] Lv Y, Lei L, Sun L. Effect of shot peening on the fatigue resistance of laser surface melted 20CrMnTi steel gear. Materials Science and Engineering: A 2015;629:8–15. doi:10.1016/j.msea.2015.01.074.

[13] Xu Z, Dunleavey J, Antar M, Hood R, Soo SL, Kucukturk G, et al. The influence of

shot peening on the fatigue response of Ti-6Al-4V surfaces subject to different machining processes. International Journal of Fatigue 2018;111:196–207. doi:10.1016/j.ijfatigue.2018.02.022.

[14] Namjoshi SA, Jain VK, Mall S. Effects of Shot-Peening on Fretting-Fatigue Behavior of Ti-6Al-4V. Journal of Engineering Materials and Technology 2002;124:222. doi:10.1115/1.1448323.

[15] Majzoobi GH, Abbasi F. On the effect of shot-peening on fretting fatigue of Al7075-T6 under cyclic normal contact loading. Surface and Coatings Technology 2017;328:292–303. doi:10.1016/j.surfcoat.2017.08.067.

[16] Tekeli S. Enhancement of fatigue strength of SAE 9245 steel by shot peening. Materials Letters 2002;57:604–8. doi:10.1016/S0167-577X(02)00838-8.

[17] Zhang X, Liu D. Effect of shot peening on fretting fatigue of Ti811 alloy at elevated temperature. International Journal of Fatigue 2009;31:889–93. doi:10.1016/j.ijfatigue.2008.10.004.

[18] Li G, Qu S, Xie MX, Li X. Effect of ultrasonic surface rolling at low temperatures on surface layer microstructure and properties of HIP Ti-6Al-4V alloy. Surface and Coatings Technology 2017;316:75–84. doi:10.1016/j.surfcoat.2017.01.099.

[19] Liu D, Liu D, Zhang X, Liu C, Ao N. Surface nanocrystallization of 17-4 precipitation-hardening stainless steel subjected to ultrasonic surface rolling process. Materials Science and Engineering: A 2018;726:69–81. doi:10.1016/j.msea.2018.04.033.

[20] Zhang Q, Hu Z, Su W, Zhou H, Liu C, Yang Y, et al. Microstructure and surface properties of 17-4PH stainless steel by ultrasonic surface rolling technology. Surface and Coatings Technology 2017;321:64–73. doi:10.1016/j.surfcoat.2017.04.052.

[21] Liu Y, Zhao X, Wang D. Determination of the plastic properties of materials treated by ultrasonic surface rolling process through instrumented indentation. Materials Science and Engineering: A 2014;600:21–31. doi:10.1016/j.msea.2014.01.096.

[22] Li G, Qu SG, Pan YX, Li XQ. Effects of the different frequencies and loads of ultrasonic surface rolling on surface mechanical properties and fretting wear resistance of HIP Ti–6Al–4V alloy. Applied Surface Science 2016;389:324–34. doi:10.1016/j.apsusc.2016.07.120.

[23] Wang B, Yin Y, Gao Z, Hou Z, Jiang W. Influence of the ultrasonic surface rolling process on stress corrosion cracking susceptibility of high strength pipeline steel in neutral pH environment. RSC Advances 2017;7:36876–85. doi:10.1039/C7RA05425D.

[24] Lu LX, Sun J, Li L, Xiong QC. Study on surface characteristics of 7050-T7451 aluminum alloy by ultrasonic surface rolling process. International Journal of Advanced Manufacturing Technology 2016;87:2533–9. doi:10.1007/s00170-016-8659-4.

[25] Wang Z, Xiao Z, Huang C, Wen L, Zhang W. Influence of Ultrasonic Surface Rolling on Microstructure and Wear Behavior of Selective Laser Melted Ti-6Al-4V Alloy. Materials (Basel) 2017;10:1203. doi:10.3390/ma10101203.

[26] Liu C, Liu D, Zhang X, Yu S, Zhao W. Effect of the Ultrasonic Surface Rolling Process on the Fretting Fatigue Behavior of Ti-6Al-4V Alloy. Materials (Basel) 2017:10:833. doi:10.3390/ma10070833.

[27] Ting W, Dongpo W, Gang L, Baoming G, Ningxia S. Investigations on the nanocrystallization of 40Cr using ultrasonic surface rolling processing. Applied Surface Science 2008;255:1824–9. doi:10.1016/j.apsusc.2008.06.034.
[28] Carlsson S, Larsson PL. On the determination of residual stress and strain fields by sharp indentation testing. PartI: theoretical and numerical analysis. Acta Materialia 2001:13.
[29] Liu C, Liu D, Zhang X, Yu S, Zhao W. Effect of the Ultrasonic Surface Rolling Process on the Fretting Fatigue Behavior of Ti-6Al-4V Alloy. Materials (Basel) 2017;10:833. doi:10.3390/ma10070833.
[30] Yasuoka M, Wang P, Zhang K, Qiu Z, Kusaka K, Pyoun YS, et al. Improvement of the fatigue strength of SUS304 austenite stainless steel using ultrasonic nanocrystal surface modification. Surface and Coatings Technology 2013;218:93–8. doi:10.1016/j.surfcoat.2012.12.033.
[31] Qin H, Ren Z, Zhao J, Ye C, Doll GL, Dong Y. Effects of ultrasonic nanocrystal surface modification on the wear and micropitting behavior of bearing steel in boundary lubricated steel-steel contacts. Wear 2017;392–393:29–38. doi:10.1016/j.wear.2017.09.012.
[32] Zhang H, Chiang R, Qin H, Ren Z, Hou X, Lin D, et al. The effects of ultrasonic nanocrystal surface modification on the fatigue performance of 3D-printed Ti64. International Journal of Fatigue 2017;103:136–46. doi:10.1016/j.ijfatigue.2017.05.019.
[33] Ting W, Dongpo W, Gang L, Baoming G, Ningxia S. Investigations on the nanocrystallization of 40Cr using ultrasonic surface rolling processing. Applied Surface Science 2008;255:1824–9. doi:10.1016/j.apsusc.2008.06.034.
[34] Liu Y, Wang L, Wang D. Finite element modeling of ultrasonic surface rolling process. Journal of Materials Processing Technology 2011;211:2106–13. doi:10.1016/j.jmatprotec.2011.07.009.
[35] Mutoh Y, Xu JQ. Fracture mechanics approach to fretting fatigue and problems to be solved. Tribology International 2003;36:99–107. doi:10.1016/S0301-679X(02)00136-6.
[36] Endo K, Goto H. Initiation and propagation of fretting fatigue cracks. Wear 1976;38:311–24. doi:10.1016/0043-1648(76)90079-X.
[37] Zhang P, Li SX, Zhang ZF. General relationship between strength and hardness. Materials Science and Engineering A 2011;529:62–73. doi:10.1016/j.msea.2011.08.061.
[38] Yang Q, Zhou W, Gai P, Zhang X, Fu X, Chen G, et al. Investigation on the fretting fatigue behaviors of Ti-6Al-4V dovetail joint specimens treated with shot-peening. Wear 2017;372–373:81–90. doi:10.1016/j.wear.2016.12.004.
[39] Guo YB, Warren AW, Hashimoto F. The basic relationships between residual stress, white layer, and fatigue life of hard turned and ground surfaces in rolling contact. CIRP Journal of Manufacturing Science and Technology 2010;2:129–34. doi:10.1016/j.cirpj.2009.12.002.
[40] Yongshou L, Xiaojun S, Jun L, Zhufeng Y. Finite element method and experimental investigation on the residual stress fields and fatigue performance of cold expansion hole. Materials and Design 2010;31:1208–15. doi:10.1016/j.matdes.2009.09.031.

[41] Amanov A, Cho IS, Kim DE, Pyun YS. Fretting wear and friction reduction of CP titanium and Ti-6Al-4V alloy by ultrasonic nanocrystalline surface modification. Surface and Coatings Technology 2012;207:135–42. doi:10.1016/j.surfcoat.2012.06.046.

[42] Kumar SA, Sundar R, Raman SGS, Kumar H, Gnanamoorthy R, Kaul R, et al. Fretting Wear Behavior of Laser Peened Ti-6Al-4V. Tribology Transactions 2012;55:615–23. doi:10.1080/10402004.2012.686087.

[43] Fridrici V, Fouvry S, Kapsa P, Perruchaut P. Prediction of cracking in Ti-6Al-4V alloy under fretting-wear: Use of the SWT criterion. Wear 2005;259:300–8. doi:10.1016/j.wear.2004.11.026.

[44] Waterhouse RB, Trowsdale a J. Residual stress and surface roughness in fretting fatigue. Journal of Physics D: Applied Physics 2000;25:A236–9. doi:10.1088/0022-3727/25/1A/036.

[45] Liu D, Tang B, Zhu X, Chen H, He J, Celis JP. Improvement of the fretting fatigue and fretting wear of Ti6Al4V by duplex surface modification. Surface and Coatings Technology 1999;116–119:234–8. doi:10.1016/S0257-8972(99)00279-0.

[46] Cadario A, Alfredsson B. Influence of residual stresses from shot peening on fretting fatigue crack growth. Fatigue and Fracture of Engineering Materials and Structures 2007;30:947–63. doi:10.1111/j.1460-2695.2007.01165.x.

[47] Lee H, Jin O, Mall S. Fretting fatigue behaviour of shot-peened Ti-6Al-4V at room and elevated temperatures. Fatigue and Fracture of Engineering Materials and Structures 2003;26:767–78. doi:10.1046/j.1460-2695.2003.00677.x.

[48] Lee H, Mall S. Fretting behavior of shot peened Ti-6Al-4V under slip controlled mode. Wear 2006;260:642–51. doi:10.1016/j.wear.2005.03.022.

[49] Lee H, Mall S. Analysis of fretting fatigue of cavitation shotless peened Ti-6Al-4V. Tribology Letters 2010;38:125–33. doi:10.1007/s11249-010-9581-9.

[50] Fu Y, Loh NL, Batchelor AW, Liu D, Xiaodong Zhu, He J, et al. Improvement in fretting wear and fatigue resistance of Ti-6Al-4V by application of several surface treatments and coatings. Surface and Coatings Technology 1998;106:193–7. doi:10.1016/S0257-8972(98)00528-3.

[51] Szolwinski MP, Farris TN. Mechanics of fretting fatigue crack formation. Wear 1996;198:93–107. doi:10.1016/0043-1648(96)06937-2.

[52] Zuo Y, Wang H, Xiong J. The aspect ratio of surface grooves and metastable pitting of stainless steel. Corrosion Science 2002;44:25–35. doi:10.1016/S0010-938X(01)00039-7.

Highlights:

1. A plastically deformed layer was generated on the surface of USRP-treated 300M steels that resulted in higher hardness.
2. USRP induced high magnitude compressive residual stress that contributed to the improvement of fretting fatigue resistance of 300M steel.
3. USRP significantly reduced the surface defects that increased the corrosion resistance of 300M steel.
4. USRP simultaneously increased in the fretting fatigue and corrosion fatigue properties of 300M steel.